ISBN: 978-3-95450-208-0 doi:10.18429/JACoW-IPAC2019-TUPTS091

PHYSICS OF ELECTRON BEAM GENERATION AND DYNAMICS FROM DIAMOND FIELD EMITTER ARRAYS

C.-K. Huang*, H. L. Andrews, R. C. Baker, R. L. Fleming, D. Kim,
T. J. T. Kwan, V. Pavlenko, A. Piryatinski, and E. I. Simakov
Los Alamos National Laboratory, Los Alamos, NM, USA 87545

Abstract

Many applications such as compact accelerators and electron microscopy demand high brightness electron beams with small beam size and low emittance. Electric-field-assisted diamond emitters manufactured from semiconductor processes are strong candidates for cathodes in such sources. The micro-scale pyramid structure of the emitter has the desirable attribute of significant field enhancement at the sharp interfaces (apex and edges) to facilitate electron emission. We use the LSP particle-in-cell code to simulate the diamond emitter in a diode setup and obtain the beam size and divergence. An empirical fit of the fields around the apex is extracted for detail study. The trend of the beam divergence observed in the simulation is further corroborated using electron's trajectory in the empirical field model.

INTRODUCTION

A Dielectric Laser Accelerator (DLA) [1] is envisioned to deliver extraordinary acceleration gradients above 300 MV/m for up to 10 fC electron bunches with femtosecond bunch length, nanometer normalized emittance, and kHz repetition rates. A compact electron source is one of the foundation technologies that needs to be developed and integrated into a prototype tabletop DLA. Such a source may also find applications for the improvement of electron microscopy and associated imaging and scattering applications. The diamond field emitter [2] — a miniaturized, high-current low-emittance cathode, offers many advantages for the compact DLA. We have conducted computation modeling to understand the emission characteristic [3] and the beam dynamics for the beam emitted from the diamond field emitter. Through 3D finite-element simulations with nanometer resolution, the dependence of the field enhancement on the shape of the emitter are determined with high accuracy. It has been shown that for the diamond emitter in a diode setup, the beam formation and acceleration is of 1D nature, except for a small region near the apex of the emitter. Using the three dimensional finite-difference-time-domain fully electromagnetic particle-in-cell code LSP, the beam dynamics are simulated in 3D with existing Murphy-Good or Child-Langmuir emission laws. The macroscopic observables, such as the beam size and divergence, are extracted. In this paper, we focus on the understanding of these observables from simulations.

* huangck@lanl.gov

LSP SIMULATION

Details of the simulations can be found in [3], here we briefly describe the simulation setup. The simulation was done in a cylindrical geometry using a diode setup with the emitter as cathode. The pyramid has a square base with a 10 μm edge and a height of 10 μm, and the anode-cathode (AK) gap is 33 μm with a nominal electric field of 12.1 V/μm at the surface of the pyramid in the absence of field enhancement. Additionally, we approximate the pyramid as a cone in r and z in the next section to exploit its azimuthal symmetry for the fields near the emitter.

Effects of External Magnetic Field on Beam Size

We explore through simulations the impact of an externally imposed magnetic field in the diode region to control the electron divergence during the beam formation process. A constant axial magnetic field is applied. In Fig. 1, the beam radius at the anode from the simulations is shown as a function of the external magnetic field strength. Though its radius shows a monotonically decreasing dependence on the field, it takes a significant field strength of 15 kG to reduce the radius by about 20% which translates into a 40% decrease in beam spot. Correspondingly in Fig. 2, the radial velocity of the electron beam is plotted against the field strength and it shows a significant decrease as the field magnitude increases. As the electron beam propagates forward, we can expect the beam spot expansion can be reasonably controlled by a strong magnetic field although its implementation in the diode design may post some challenges.

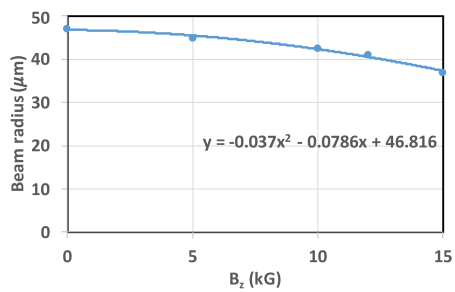

Figure 1: Beam radius vs. magnetic field strength.

FIELDS NEAR THE EMITTER

To understand the electron dynamics from the diamond field emitter in the diode setup, it is essential to investigate the fields around the emitter. The pyramidal base is expected to have field enhancement at the edges, making the field

ISBN: 978-3-95450-208-0 doi:10.18429/JACoW-IPAC2019-TUPTS091

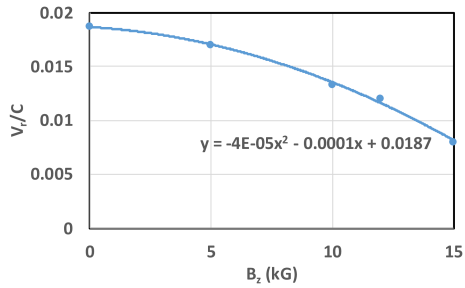

Figure 2: Beam radial velocity vs. magnetic field strength.

distribution more complicated. However, it is informative to first investigate a cylindrically symmetric cone emitter and show a general analytic approach to obtain the fields around the tip and an empirical relation from our simulation. An electron's trajectory is then considered in such fields.

Model for a Cone-Shape Emitter in a Diode

Previous work by Chung et al. [4] has investigated the general solution of the Laplace's equation applicable to an azimuthal symmetric setup of an infinite planar anode and a cone tip cathode separated by a distance d. This resembles the geometry of the diamond emitter in our experiment. The solution of the Laplace equation in spherical coordinates (R, θ, ϕ) for the electrostatic potential between the cone tip and the anode has the following form,

$$V(R,\theta) = \Sigma_\nu \left(A_\nu R^\nu + B_\nu R^{-\nu-1} \right) P_\nu(\cos\theta), \qquad (1)$$

where R is the radius from the cone apex, θ is the polar angle measured from the symmetric axis z pointing from the cone apex to the anode, ϕ is the azimuthal angle. $P_\nu(x)$ is the Legendre polynomial of order ν, and A_ν, B_ν are constant coefficients. The general solution is subjected to the boundary conditions, i.e., $V = 0$ and $V = V_0$ at the cathode and anode, respectively. However, it should be noted that the cathode in this model geometry is the whole cone surface $(\theta = \theta_c)$, therefore $V(\theta = \theta_c) = 0$, while our geometry has an micron-scale emitter on top of a much larger planar surface for the cathode. Thus, the former is only a reasonable approximation to our geometry for the field very close to the cone apex. With this boundary condition, the choice of ν in Eq. 1 is limited to $\nu = \nu_c$, where ν_c is the solution of $P_{\nu_c}(\cos\theta_c) = 0$.

For a special case where the cone apex nearly touches the anode ($d \to 0$), an analytic solution is known, i.e., $V_{contact}(R,\theta) = V_0\,[\ln(\tan(\theta/2))/\ln(\tan(\theta_c/2))]$.

For a more general (non-touching) case, Chung et al. proposed to match the potential $V_{contact}$ for the touch case at a sufficiently large radius R_c to determine A_ν, B_ν in Eq. 1. This method is in principle applicable to our problem setup, e.g., by matching the boundary conditions at the planar anode and cathode. However, as shown in [3], the solution of the potential in our diode setup is predominantly of uniform 1D nature with a strong field enhancement only near the micron-scale emitter. For such case, successfully matching the boundary conditions may require many terms in Eq. 1.

Numerical Fit to the Fields Near the Emitter

An empirical approach is instead used to characterize the fields near the conic emitter. Here, we modeled the emitter in 2D (r, z) cylindrical symmetric LSP simulation. The cone has a height of 5 μm and the base radius is 2.5 μm, corresponding to a half opening angle of $\theta_c = \text{atan}(2.5/5.0)$. The cone apex is at $(r = 0, z = 0)$, where we also define spherical coordinates (R, θ) as in the previous section. The steady state electric fields in the simulation in (r, z) coordinate, after subtracting the uniform field $E_{z0} = 11.4$ V/μm in the diode without the emitter, are projected to (R, θ) directions. Figs. 3 and 4 show the projected fields E_R and E_θ. Simple functional fits are found to these fields and they are shown in Figs. 3 and 4 as solid lines. These fits are satisfactory for positions not too close to the apex and θ not too close to $(\pi - \theta_c)$ (where the fields may be affected by simulation resolution). For E_R, the fit is only a function of R, not θ, while for E_θ a linear dependence on θ is found. Note that these functional fits may be improved by the divergence-free condition but such improvement is not essential to the electron dynamics presented in the next section.

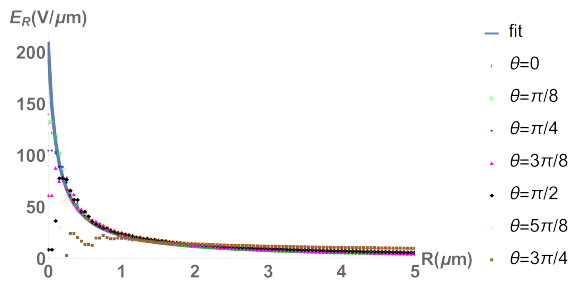

Figure 3: E_R (symbols) as a function of the distance R to the emitter apex for various polar angle θ and the functional fit (blue line). The fit is $E_R[\text{V}/\mu\text{m}] = 25/(R[\mu\text{m}] + 0.12)$.

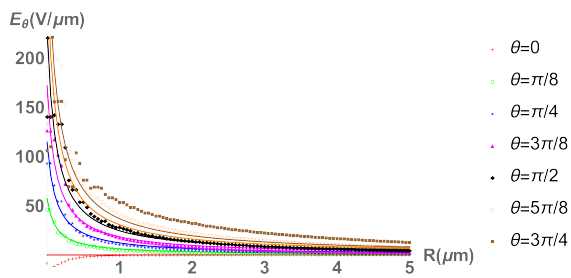

Figure 4: E_θ (symbols) as a function of R for various polar angle θ and their functional fits (solid lines of corresponding colors). The fit is $E_\theta[\text{V}/\mu\text{m}] = 1.1 \times (\theta/(\pi/2)) \times 25/(R[\mu\text{m}] + 0.12)$.

ANALYSIS OF BEAM DIVERGENCE

With the functional fits of the fields, the trajectory of an electron emitted with initial longitudinal and transverse

ISBN: 978-3-95450-208-0 doi:10.18429/JACoW-IPAC2019-TUPTS091

velocities v_{z0} and v_{r0} from the cathode can be numerically integrated. For simplicity, we only consider an electron emitted from the tip apex ($z_0 = 0, r_0 = 0$) and no emission law is invoked. Figure 5 shows the longitudinal and transverse velocities $v_z(t)$ and $v_r(t)$ shortly after the electron is emitted for two cases. In the first case, $v_{r0} \approx 103\,\mu$m/ns is taken, corresponding to the thermal velocity at temperature $T = 300$ K, while $v_{z0} = v_{z0}/10$, to mimic emission mostly in the transverse direction. In the second case, $v_{r0} = v_{z0} = 103\,\mu$m/ns, which represents a more isotropic emission. In both cases, v_r quickly reaches saturation as the electron moves away from the apex. While v_z increases rapidly during this time, it increases at a lower but linear rate in the region with more uniform field when $t > 0.003$ ns. v_{z0} has a large effect on the saturated value of v_r, as shown in Fig. 5. The smaller v_r in case 2 can be understood by the fact that the electron spends much less time in the region with enhanced fields, therefore has smaller transverse momentum gain.

Such effect can eventually lead to smaller electron divergence angle $\delta = v_r/v_z$ for the latter part of the trajectory. Figure 6 indicates that, although δ decreases quite substantially in both cases when the electron moves across the diode, case 2 has always a smaller divergence at the same longitudinal location. The final divergence at $z = 3 \sim 4$ mm where the anode is located in our experimental setup is about $2 \sim 3.5°$, which is consistent with the measurements. Finally, it should be noted that the solution to electron's equation of motion is self-similar if the fields in the diode are scaled by a factor β (i.e., voltage across AK gap is scaled by β but with gap distance fixed) and the initial velocities (energies) are scaled by $\beta^{1/2}$ (β). The electron divergence in such case is shown in Fig. 6 to be the same as the unscaled case. Therefore, increasing the AK voltage will have little effect on the divergence angle when the electron emission energy is scaled by the same factor. On the other hand, Fig. 6 indicates that extending the AK gap while keeping the field strength in the gap can further reduce the divergence angle.

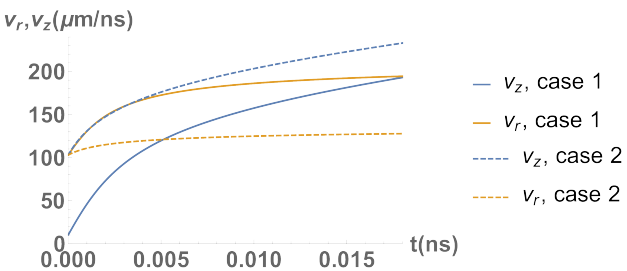

Figure 5: Evolution of v_r and v_z for the early part of the trajectory for two cases with different v_{z0} (see text).

CONCLUSION

We have presented simulation results and corresponding analysis for the beam formation from a micron-scale diamond emitter in a planar diode setup. The 1D accelerating structure leads to small beam size, despite large divergence angle near the emitter. The divergence is mainly determined by the diode geometry, however, it has been shown that initial emission conditions and magnetic field can also affect beam size and divergence. Recently, we have also developed a first-principle model of Monte Carlo electron transport [3] inside the emitter and their subsequent emission across the vacuum interface based on their calculated tunneling probability. A nano-scale tip that may be present at the top of the pyramid can further enhance external fields and beam emission, as well as introduces electronic structure size quantization affecting the transport and tunneling processes within the tip [5]. In the future, we will apply a more comprehensive emission model that includes such effects to the simulations of diamond field emitters for detail comparison with experiments.

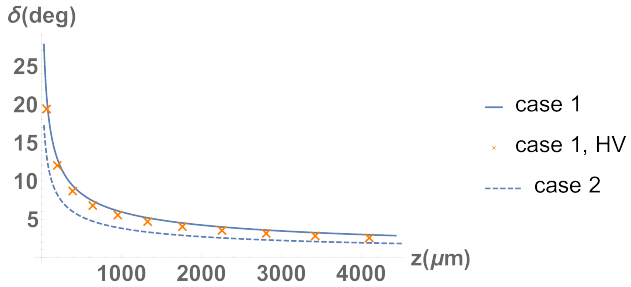

Figure 6: Evolution of the electron divergence angle as a function of distance for case 1, 2 and the case similar to case 1 but with fields and initial electron energy scaled by $\beta = 3$ (denoted "case 1, HV").

ACKNOWLEDGMENTS

Work in this paper was supported by the Laboratory Directed Research and Development program of Los Alamos National Laboratory under project 20170006DR. One of the authors (TK) would like to acknowledge useful discussions on LSP simulations with Dale Welch and Dave Rose.

REFERENCES

[1] R. J. England *et al.*, "Dielectric laser accelerators", *Reviews of Modern Physics*, vol. 86, no. 4, pp. 1337–1389, Dec. 2014.

[2] E. I. Simakov, H. L. Andrews, M. J. Herman, K. M. Hubbard, and E. Weis, "Diamond field emitter array cathodes and possibilities of employing additive manufacturing for dielectric laser accelerating structures", *AIP Conference Proceedings*, vol. 1812, 2017, ISSN: 15517616.

[3] C.-K. Huang *et al.*, "Modeling of diamond field emitter arrays for a compact source of high brightness electron beams", *Journal of Applied Physics*, vol. 125, no. 16, p. 164 501, 2019.

[4] M. Chung, P. H. Cutler, T. E. Feuchtwang, and N. M. Miskovsky, "Solution of laplace's equation for a rigid conducting cone and planar counter-electrode : comparison with the solution to the Taylor conical model of a field emission LMIS", *Le Journal de Physique Colloques*, vol. 45, no. C9, pp. C9–145–C9–152, 1984.

[5] A. Piryatinski, C.-K. Huang, and T. J. T. Kwan, "Theory and simulations of electron transport and emis-sion from a semiconductor nanotip", *Journal of Applied Physics, in press*, 2019. arXiv:1901:02183